Journal of Electroceramics 5:3, 191–199, 2000

Relaxor Behavior of $(Sr_{0.8}Ba_{0.2})TiO_3$ Ceramic Solid Solution Doped with Bismuth

LIQIN ZHOU, P.M. VILARINHO & J.L. BAPTISTA
Department of Ceramics and Glass Engineering, UIMC, University of Aveiro, 3810 Aveiro, Portugal

Submitted April 22, 1999; Revised March 23, 2000; Accepted May 15, 2000

Abstract. The dielectric properties of $(Sr_{0.8}Ba_{0.2})_{1-1.5x}Bi_xTiO_3$ ceramics in the range $0 \leq x \leq 0.18$ are investigated. A ferroelectric relaxor behavior is observed. The degree of the diffuseness and the relaxation of the phase transition increases as the Bi content increases. A random electric field is suggested to be responsible for the relaxor behavior observations. The dependence of the diffuseness on the grain size is presented.

Keywords: barium strontium titanate, relaxor, dielectric properties

1. Introduction

The so-called ferroelectric relaxor behavior, characterized by a diffuse phase transition (DPT), a strong frequency dispersion of the dielectric properties and an absence of macroscopic polarization and anisotropy at temperatures far below T_{max} (the temperature of the dielectric permittivity maximum), was first discovered in $Ba(Ti_{1-x}Sn_x)O_3$ solid solutions [1]. Later, many perovskites and tungsten bronzes, namely lead-based complex compounds and $BaTiO_3$-based solid solutions, were found to show ferroelectric relaxor behavior, e.g., $Pb(Mg_{1/3}Nb_{2/3})O_3$ (PMN) [2], $Pb(Sc_{1/2}Ta_{1/2})O_3$ (PST) [3], $Pb(Fe_{2/3}W_{1/3})O_3$ (PFW) [4,5], $Ba(Ti,Zr)O_3$ [6] and $Ba(Ti,Hf)O_3$ [7].

The polarization mechanism of ferroelectric relaxors is believed to be different from that of normal ferroelectrics. At different times and following progressive experimental evidences many models have been proposed. The first was the compositional fluctuation model by Smolenskii [8]. This model proposed that the DPT was caused by the chemical inhomogeneity arising from the random distribution of more than one type of cation at the same sites [8]. This postulation was later somewhat confirmed by Setter et al. [3], who observed that highly B site cation ordered PST ceramics showed a normal ferroelectric phase transition whereas a disordered one exhibited the characteristics of a relaxor. Nano-scale ordered regions were observed by TEM in some relaxors [9–11]. Cross proposed a superparaelectric model [12], analogous to superparamagnetism. The dielectric relaxation was believed to occur due to thermally activated polarization reversals between identical crystallographic directions [12]. The superparaelectric model attributed the relaxor behavior to a cluster size effect [12]. Later, Viehland extended the ''superparaelectric'' concept proposing a dipolar glass model [13]. It was suggested that the ferroelectric relaxor can be considered as a system with interacting superparaelectric moments [13]. In addition, a random-electric-field model was suggested for PMN by Westphal [14]. In this model, it was suggested that the ferroelectric relaxor can be regarded as a ferroelectric domain state, its diffuseness being due to quenched random electric fields originated from charge fluctuations [14]. Recently, the observation that the size of the domains and the degree of B cation order of $Pb(Mg_{1/3}Ta_{2/3})O_3$ (PMT) [15] can be significantly increased by annealing at high temperatures has attracted particular attention. These ceramics that were comprised of large domains still retained the relaxor behavior [15].

Strontium titanate ($SrTiO_3$) is a quantum paraelectric which shows high dielectric permittivity at

low temperature with no ferroelectric phase transition occurring down to near 0 K [16]. However, a relaxation behavior, somewhat similar to that observed in ferroelectric relaxors, was also observed in its solid solutions such as $Sr_{1-x}Ca_xTiO_3$ [17] and $Sr_{1-1.5x}Bi_xTiO_3$ [18,19]. It was suggested that Ca^{2+} or Bi^{3+} ions are located at off-center positions of A sites [17,19]. The relaxation of these systems was attributed to a random field induced domain state [17,19].

Barium titanate ($BaTiO_3$) is known as a typical ferroelectric material. Ferroelctric relaxor behavior was observed in many of $BaTiO_3$-based solid solutions such as $Ba(Ti,Sn)O_3$ [1], $Ba(Ti,Zr)O_3$ [6] and $Ba(Ti,Hf)O_3$ [7]. For $Sr_xBa_{1-x}TiO_3$ solid solutions, ferroelectric relaxor behavior was observed only in $SrTiO_3$ rich side ($x > 0.80$) and the solid solutions with $x \leq 0.80$ showed normal ferroelectric behavior [20,21]. The relaxor behavior of $Sr_xBa_{1-x}TiO_3$ solid solutions can not be attributed to the same mechanism as that of $Sr_{1-x}Ca_xTiO_3$ and $Sr_{1-1.5x}Bi_xTiO_3$ since Ba^{2+} has a bigger ionic radius compared to Sr^{2+} [22] and thus could not be an off-center ion [21]. The physical nature of the relaxor behavior in lead-based complex compounds or in $BaTiO_3/SrTiO_3$-based solid solutions is still controversial.

In the present work, the dielectric properties of $(Sr_{0.8}Ba_{0.2})TiO_3$ ceramic solid solution doped with different amounts of bismuth up to 18 at % are investigated. The ferroelectric-paraelectric phase transition of $(Sr_{0.8}Ba_{0.2})TiO_3$ ceramics are found to get diffused and relaxed for increasing amounts of the Bi doping. The possible mechanisms responsible for the diffuseness phenomena are discussed.

2. Experimental

Ceramic samples were prepared by the conventional mixed oxide method. Reagent grade $SrCO_3$, $BaCO_3$, TiO_2 and Bi_2O_3 were weighed according to the composition $(Sr_{0.8}Ba_{0.2})_{1-1.5x}Bi_xTiO_3$ where $x = 0$, 0.002, 0.005, 0.007, 0.01, 0.03, 0.05, 0.07, 0.1, 0.12, 0.14, 0.16 and 0.18, respectively. We admit that A site (strontium and/or barium) vacancies were introduced as $[(Sr_{0.8}Ba_{0.2})_{1-1.5x}Bi_x(V_A)_{0.5x}]TiO_3$ to balance the charge misfit due to the substitution of divalent Sr^{2+} and/or Ba^{2+} ions by trivalent Bi^{3+} ions. After ball-milled in alcohol for 6 h using agate pots and agate balls in a planetary mill, the powders were dried, and then calcined between 950°C and 1200°C for 6 h; the higher the Bi content, the lower the calcination temperature. The calcined powders were milled again for 8–10 h, to obtain powders of less than 5 μm of particle size. Pellets of 10 mm in diameter and 2–3 mm in thickness were uniaxially pressed at 100 MPa and then isostatically pressed at 250 MPa. The sintering was conducted at 1350, 1350, 1350, 1350, 1320, 1320, 1300, 1280, 1250, 1220, 1180, 1150 and 1100°C corresponding to $x = 0$, 0.002, 0.005, 0.007, 0.01, 0.03, 0.05, 0.07, 0.1, 0.12, 0.14, 0.16 and 0.18, respectively for 4 h, followed by a furnace cooling. The sintering conditions had to be adjusted for each sample composition to obtain high relative densities.

Some of the sintered samples were ground into powder and the phases were identified by X-ray diffraction analysis. The scanning electron microscopy (SEM) microstructures of the samples were observed in polished sections using a Hitachi S4100 microscope. Grain size measurements were made on SEM photographs using the intercept method.

For the dielectric measurements, sintered samples were polished and gold electrodes were sputtered on both sides. Dielectric permittivity was measured, at different frequencies between 100 Hz and 1 MHz, as a function of temperature, using a Solartron 1260 Impedance/Gain-Phase Analyzer and a Displex APD-Cryogenics cryostat during heating up at a rate of 1 K/min in the temperature range of 12–320 K. Measurements in the range of 320–400 K were done in a furnace during heating up at a rate of 1 K/min. The data were taken every 2 K. The dielectric permittivity curve for each frequency was then smoothed and interpolated to determine the temperature of the permittivity maximum as accurately as possible.

3. Results

The X-ray diffraction patterns of $(Sr_{0.8}Ba_{0.2})_{1-1.5x}Bi_xTiO_3$ for $x = 0.1$, 0.12 and 0.16 are shown in Fig. 1. Single phase cubic perovskite was obtained up to $x = 0.1$ under the sintering conditions used in this work. When the amount of bismuth exceeds 10 at % (i.e., $x > 0.1$), some extra peaks appeared in the X-ray diffraction patterns. These extra peaks are assignable to $Bi_2Ti_2O_7$. The amount of the

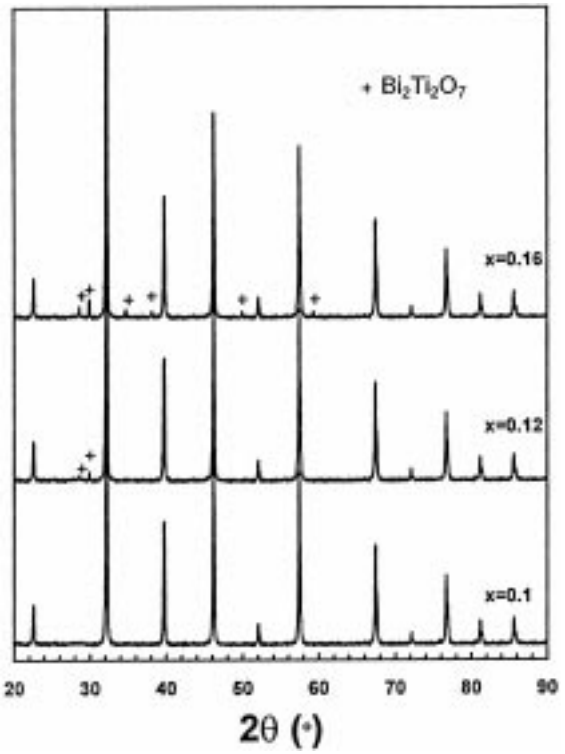

Fig. 1. X-ray diffraction patterns of $(Sr_{0.8}Ba_{0.2})_{1-1.5x}Bi_xTiO_3$ ceramics for $x = 0.1, 0.12$ and 0.16.

$Bi_2Ti_2O_7$ phase increases as the bismuth content increases.

The samples with high percentage of Bi and sintered at lower temperatures had a smaller grain size. The average grain size for each studied composition determined from SEM photographs is shown in Table 1. When $x > 0.1$, a long needle shaped second phase appeared, as can be seen in Fig. 2. X-ray energy dispersive analysis of this second phase indicated that this phase is enriched with titanium and bismuth. According to the X-ray results (Fig. 1), this phase is $Bi_2Ti_2O_7$.

Evident hysteresis loops were observed in all the studied compositions, indicative of a ferroelectric state. Figure 3 shows the hysteresis loops of some compositions.

Figure 4 shows the temperature dependence of the dielectric permittivity at various frequencies for the $x = 0$, 0.01, 0.05, 0.1, 0.12 and 0.18 compositions. The dielectric permittivity curves are sharp and the temperatures of the permittivity maxima are frequency independent for the pure $Sr_{0.8}Ba_{0.2}TiO_3$ solid solution. As the Bi content increases, the permittivity curves become round with frequency dispersion. The dielectric permittivity maximum values $(\varepsilon_{r\max})$ at 1 kHz for all the compositions as well as the maximum temperatures $(T_{\max})$ are shown in Table 1. $\varepsilon_{r\max}$ decreases with the increase in the Bi content. The compositional dependence of $T_{\max}$ is plotted in Fig. 5a where it can be seen that $T_{\max}$ increases linearly up to $x = 0.10$.

It is well known that the dielectric permittivity of a classic ferroelectric above the Curie temperature follows the Curie-Weiss law, described by:

$$\varepsilon_r = c(T - \Theta)^{-1} \tag{1}$$

where ε_r is the dielectric permittivity at T, c the Curie-Weiss constant, and Θ the Curie-Weiss temperature. However, the dependence of the dielectric permittivity of DPT ferroelectrics on temperature, above the Curie temperature, differs from the Curie-Weiss law over a wide temperature range.

Figure 6 depicts the reciprocal permittivity $(1/\varepsilon_r)$ at 1 kHz versus temperature for $x = 0$ and $x = 0.12$ compositions. The curve can be fitted to the Curie-Weiss law at $T_{\max}$ for the $x = 0$ sample while, for the $x = 0.12$ composition, a good fitting could only be obtained at temperature far above $T_{\max}$. The difference between the temperature at which the curve starts to follow the Curie-Weiss law (T_{cw}) and the $T_{\max}(\Delta T_1 = T_{cw} - T_{\max})$ can then somewhat characterize the diffuseness of the phase transition. T_{cw} values as well as ΔT_1 values for all the compositions are shown in Table 1. The variation of ΔT_1 with x is also plotted in Fig. 5b.

The diffuseness of the phase transition can be also empirically described by the parameter $\Delta T_2 = T_{0.9\varepsilon r\max(100Hz)} - T_{\varepsilon r\max(100Hz)}$, i.e., the difference between the temperature corresponing to 90% of the permittivity maximum $\varepsilon_{r\max}$ in the high temperature side and $T_{\varepsilon r\max(100Hz)}$. The ΔT_2 values are shown in Table 1 and Fig. 5c.

As can be seen in Fig. 5b and c, ΔT_1 and ΔT_2 vary with x in a very similar way. They increase as the Bi content increases up to $x = 0.10$; they do not change until $x = 0.14$ and then markedly increase.

In order to quantify the frequency dispersion of $T_{\max}$, i.e., the relaxation degree, a parameter ΔT_3 defined as $\Delta T_3 = T_{\max(1\,\mathrm{MHz})} - T_{\max(100\,\mathrm{Hz})}$ was used. ΔT_3 for the different compositions are also shown in Table 1 and Fig. 5d. ΔT_3 increases with increasing the

Table 1. Average grain size, dielectric permittivity maximum ($\varepsilon_{r\max}$) (1 kHz), temperature of the permittivity maximum ($T_{\max}$) (1 kHz), the temperature where the curve starts to follow Curie-Weiss law (T_{cw}) (1 kHz), $\Delta T_1 = T_{cw} - T_{\max}$ (1 kHz), $\Delta T_2 = T_{0.9\varepsilon r\max(100\text{ Hz})} - T_{\varepsilon r\max(100\text{ Hz})}$ and $\Delta T_3 = T_{\max(1\text{ MHz})} - T_{\max(100\text{ Hz})}$ for $(Sr_{0.8}Ba_{0.2})_{1-1.5x}Bi_xTiO_3$ ceramics

x	Grain size (μm)	$\varepsilon_{r\max}$ (at 1 kHz)	$T_{\max}$ (K) (at 1 kHz)	T_{cw}(K) (at 1 kHz)	ΔT_1 (K) (at 1 kHz)	ΔT_2 (K)	ΔT_3 (K)
0	4.0	23,310	127	127	0	—	0
0.002	3.9	18,000	129	137	8	9	0
0.005	3.7	14,500	130	149	19	13	3
0.007	3.7	13,800	131	148	17	15	4
0.01	3.3	13,170	133	154	21	14	6
0.03	2.9	6300	141	179	38	22	25
0.05	2.5	3480	154	213	59	31	33
0.07	2.2	3100	165	235	70	41	39
0.1	1.8	2960	178	265	87	50	48
0.12	1.0	1830	180	264	84	53	50
0.14	1.1	1600	181	269	88	55	50
0.16	0.6	1410	179	289	110	78	53
0.16*	1.5	1550	173	259	86	58	51
0.18	0.7	1060	179	309	130	95	51

*Sintered at 1150°C for 28 h.

Bi content up to $x = 0.1$ and then stays almost constant.

A plot of $1/T_{\max}$ versus $\ln(\omega)$ for compositions $x = 0.05$, 0.1 and 0.18 is shown in Fig. 7 where a non-linear behavior is obvious, indicating that the data do not fit the simple Debye equation,

$$\omega = \omega_0 \exp\left(\frac{-E_a}{KT_{\max}}\right) \tag{2}$$

where ω is the angular frequency, ω_0 the pre-exponential factor, E_a the activation energy, K the Boltzman constant and $T_{\max}$ the temperature of the permittivity maximum.

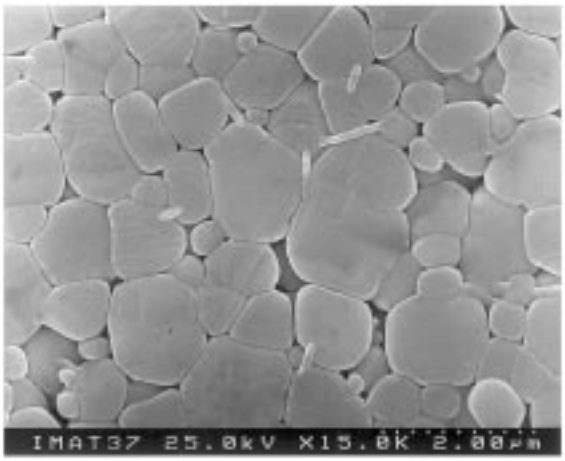

Fig. 2. SEM microstructure of $(Sr_{0.8}Ba_{0.2})_{1-1.5x}Bi_xTiO_3$ ceramics for $x = 0.12$.

The data can be well fitted to the Vogel-Fulcher relationship:

$$\omega = \omega_0 \exp\left(\frac{-E_a}{K(T_{\max} - T_f)}\right) \tag{3}$$

where T_f is the static freezing temperature. The results are shown in Fig. 8 and Table 2. A parameter ΔT_4, defined as $\Delta T_4 = T_{\max(1\text{ MHz})} - T_f$, is also listed in Table 2, for comparing the relative freezing temperatures of the various compositions. From Table 2, we can see that the activation energy is similar for the three compositions, pointing to the same process, while ΔT_4 significantly increases from 57 K for $x = 0.05$ to 75 K for $x = 0.1$ and then slightly changes to 80 K for $x = 0.18$.

Since, according to Eq. (3) the freezing temperature will tend to be coincident with $T_{\max}$ when $\omega \to 0$, the difference between $T_{\max(1\text{ MHz})}$ and T_f, ΔT_4, also somewhat reflects the degree of the frequency dispersion. ΔT_4 will then have the same trend as ΔT_3, as indeed observed (Table 2 and Table 1).

4. Discussion

X-ray and SEM results (Figs. 1 and 2) suggest that the solid solubility limit of bismuth in $(Sr_{0.8}Ba_{0.2})TiO_3$ ceramics is around 10 at % at 1250°C. The compositional dependence of $T_{\max}$ (Fig. 5(a)) shows that $T_{\max}$ increases linearly with the increase in the Bi content

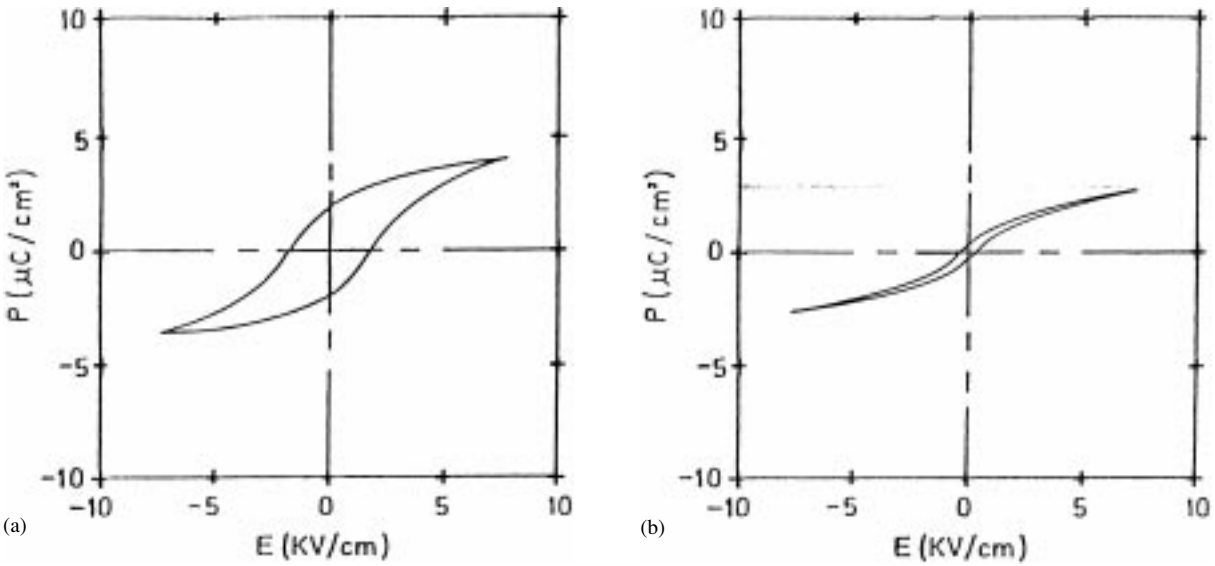

Fig. 3. Hysteresis loops at 50 Hz for $(Sr_{0.8}Ba_{0.2})_{1-1.5x}Bi_xTiO_3$ ceramics: $x = 0$ at 15 K (a) and $x = 0.18$ at 120 K (b).

up to $x = 0.1$ and keeps unchanged thereafter. This seems to indicate that the Bi ions are shifting the transition temperature to high temperatures until the solubility limit is exceeded.

First we discuss the dielectric behavior of the compositions within the solubility limit $(x \leq 0.1)$.

As can be seen in Fig. 4, undoped $(Sr_{0.8}Ba_{0.2})TiO_3$ ceramics exhibits a normal ferroelectric behavior: a sharp permittivity peak independent of frequency. However, an evident relaxor behavior is observed in Bi doped samples. The diffuseness of the phase transition (characterized by ΔT_1 and ΔT_2) and the

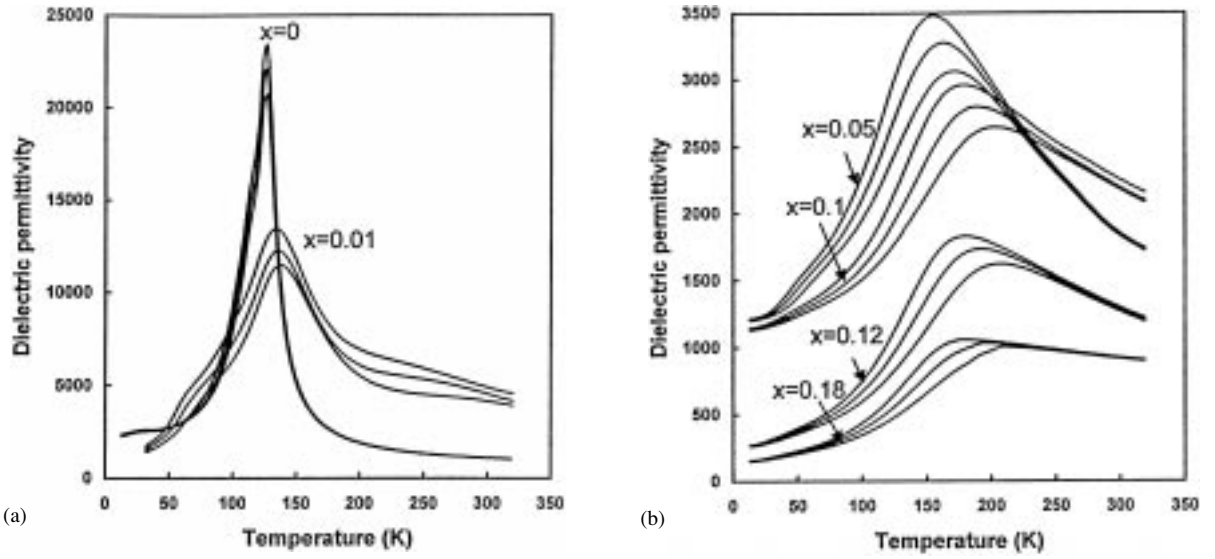

Fig. 4. Dielectric permittivity at various frequencies as a function of temperature for $(Sr_{0.8}Ba_{0.2})_{1-1.5x}Bi_xTiO_3$ ceramics where $x = 0, 0.01$ (a), 0.05, 0.1, 0.12, and 0.18 (b). The top curve corresponds to 1 kHz, the middle one to 10 kHz and the bottom one to 100 kHz.

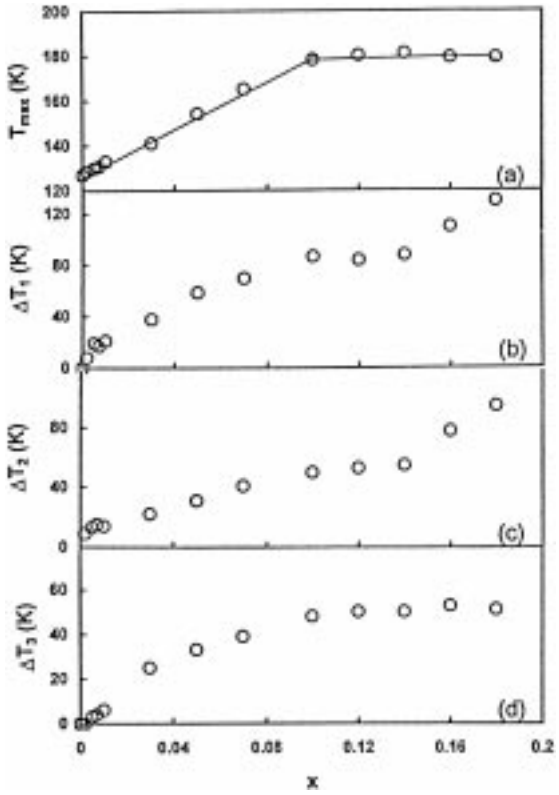

Fig. 5. The compositional dependence of T_{max}(a), ΔT_1 (b), ΔT_2 (c) and ΔT_3 (d) from Table 1.

frequency dispersion of the T_{max} (characterized by ΔT_3) significantly increase as the Bi content increases (Table 1 and Fig. 5(b), (c) and (d)).

Previous study on Bi doped $BaTiO_3$, done by the authors, showed that no dielectric diffuseness and frequency dispersion was observed within the solubility limit [23]. However, a round dielectric permittivity peak with frequency dependence was reported in Bi doped $SrTiO_3$ ceramics [18,19]. This led us to consider that the DPT behavior of Bi doped $(Sr_{0.8}Ba_{0.2})TiO_3$ has a similar nature to that of Bi doped $SrTiO_3$.

In pure $SrTiO_3$ no ferroelectric phase transition occurs at temperature down to almost 0 K [16]. However, evident hysteresis loops were observed in Bi doped $SrTiO_3$ ceramics [19], indicating that the ferroelectricity was induced by Bi doping. It was reported that at low Bi concentration (≤ 2.67 at %), Bi doped $SrTiO_3$ ceramics exhibited a quantum ferroelectric behavior while a ferroelectric relaxor behavior was observed at high Bi concentration ($>$ 2.67 at %) [19]. It was suggested that Bi ions were located at off center positions at Sr^{2+} sites [19], similarly as suggested to Ca^{2+} doped $SrTiO_3$ [17] and Li doped $KTaO_3$ [24,25]. It was also suggested that strontium vacancies (V''_{Sr}) may occur in Bi doped $SrTiO_3$ in order to balance the charge misfit caused by trivalent Bi^{3+} ions substituting divalent Sr^{2+} ions [19]. Off-center Bi^{3+} ions and $Bi^{3+} - V''_{Sr}$ centers form dipoles and thus set up local electric fields. The appearance of ferroelectric and relaxor behavior was then suggested to be a result of competition of interactions between dipoles and random electric fields [19]. In other words, the ferroelectric relaxor behavior was attributed to the random field induced domain state [19].

$(Sr_{0.8}Ba_{0.2})TiO_3$, differently from $SrTiO_3$, is a ferroelectric. For Bi doped $(Ba_{0.2}Sr_{0.8})TiO_3$, T_{max} linearly increases with the increase in the Bi content

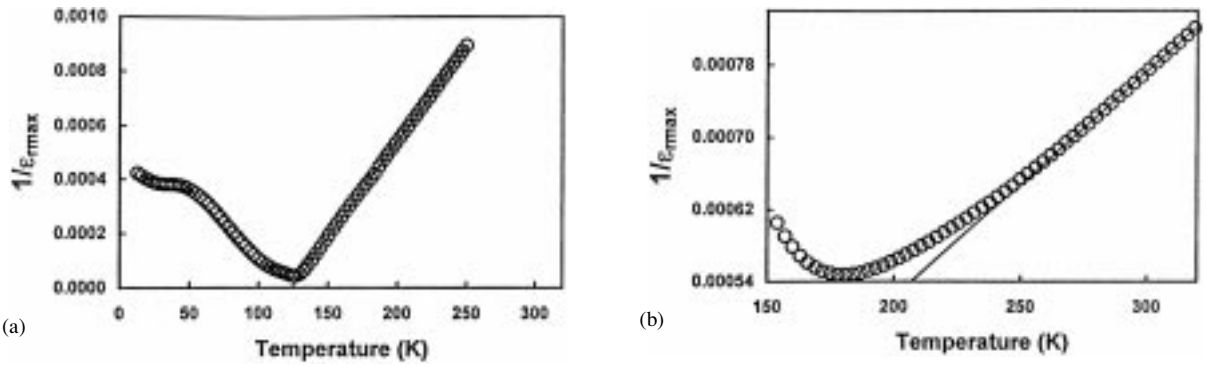

Fig. 6. The reciprocal permittivity $(1/\varepsilon_r)$ at 1 kHz as a function of temperature for $(Sr_{0.8}Ba_{0.2})_{1-1.5x}Bi_xTiO_3$ ceramics where $x = 0$ (a) and 0.12 (b). The solid line is the fitting to the Curie-Weiss law.

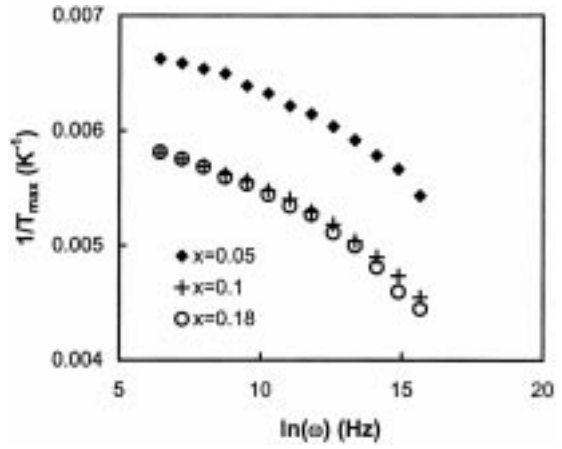

Fig. 7. $1/T_{\max}$ versus $\ln(\omega)$ for $(Sr_{0.8}Ba_{0.2})_{1-1.5x}Bi_xTiO_3$ ceramics ($x = 0.05$, 0.1 and 0.18).

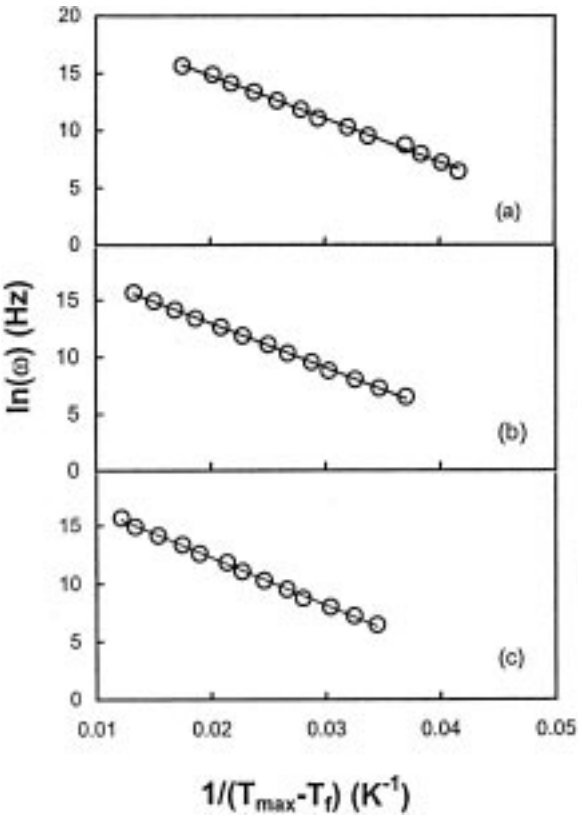

Fig. 8. $\ln(\omega)$ versus $1/(T_{\max} - T_f)$ for $(Sr_{0.8}Ba_{0.2})_{1-1.5x}Bi_xTiO_3$ ceramics: (a) $x = 0.05(T_f = 127\,K)$, (b) $x = 0.1(T_f = 145\,K)$ and (c) $x = 0.18(T_f = 143\,K)$. The solid line is the fitting to the Vogel-Fulcher relationship.

within the solubility limit (Fig. 5(a)) and the degree of the diffuseness and the relaxation of the phase transition also increases monotonously (Fig. 5b, c and d). This implies that it is the ferroelectric-paraelectric phase transition of the $(Sr_{0.8}Ba_{0.2})TiO_3$ solid solution rather than an induced domain state assumed for Bi doped $SrTiO_3$ system [19] that is gradually getting diffused and relaxed by Bi doping. Similarly as suggested for Bi doped $SrTiO_3$ [19], the Bi^{3+} ions substituting for Sr^{2+} in $(Sr_{0.8}Ba_{0.2})TiO_3$ solid solution can also be located at off-center positions and A site (strontium and/or barium) vacancies (V''_A) may also appear to compensate the charge imbalance arising from the substitution of A sites by Bi^{3+} ions. A random electric field formed by off-center Bi^{3+} ions and $Bi^{3+} - V''_A$ dipoles would then suppress ferroelectricity, accounting for the relaxor behavior of Bi doped $(Sr_{0.8}Ba_{0.2})TiO_3$ ceramics. If this explanation holds, the Bi^{3+} ions substituting for Ba^{2+} ions should not be at off-center positions since Bi doped $BaTiO_3$ does not show dielectric diffuseness and frequency dispersion [23]. It has been suggested that the substituting ions, having smaller ionic radius and greater polarization forces as compared to the lattice ions, will generally be off-center located [25]. Bi^{3+} has a smaller ionic radius compared to either Sr^{2+} or Ba^{2+} [22]. Optical measurements showed that Ba^{2+} has a higher polarizability value $(2.5 \times 10^{-24}\,cm^3)$ than $Sr^{2+}(1.6 \times 10^{-24}\,cm^3)$ [26]. The measured polarizability value for Bi^{3+} was not found. However, according to the above suggestion [25] it would seem that Bi^{3+} has a polarization force between Sr^{2+} and Ba^{2+}. Shanoon [27] calculated the polarizabilities of many ions according to the dielectric constants of their oxides and fluorides. Although the calculated values of Ba^{2+} and Sr^{2+} $(6.40 \times 10^{-24}\,cm^3$ and $4.24 \times 10^{-24}\,cm^3$ respectively) are slightly different from the measured values, the value for $Bi^{3+}(6.12 \times 10^{-24}\,cm^3)$ is indeed between the values of Ba^{2+} and Sr^{2+}.

It can also be invoked that the size mismatch of Ba^{2+}, Sr^{2+} and Bi^{3+} ions may cause a random strain field that can contribute to set up the dielectric diffuseness and relaxation of Bi doped $(Sr_{0.8}Ba_{0.2})TiO_3$ ceramics. However, it is then not easy to understand why Bi doped $BaTiO_3$ does not show dielectric diffuseness and relaxation [23] since the mismatch of Ba^{2+} and Bi^{3+} can also cause a random strain field.

Table 2. Vogel-Fulcher law fitting parameters: ω_0, activation energy E_a, freezing temperature T_f and $T_{\max(1\ \mathrm{MHz})} - T_f = \Delta T_4$ for $(Sr_{0.8}Ba_{0.2})_{1-1.5x}Bi_xTiO_3$ ceramics.

X	ω_0 (Hz)	E_a (eV)	T_f (K)	ΔT_4 (K)
0.05	4.87×10^9	0.032	127	57
0.1	1.02×10^9	0.034	145	75
0.18	7.86×10^8	0.035	143	80

When the solubility limit was exceeded $(x > 0.1)$, the diffuseness of the phase transition (ΔT_1 and ΔT_2) exhibit different behavior in different Bi concentration ranges (Fig. 5b and c). When $0.1 < x \leq 0.14$, ΔT_1 and ΔT_2 do not show any evident change with the increase of x while both markedly increased above 0.14. The frequency dispersion of $T_{\max}(\Delta T_3)$ was constant when the solubility limit was exceeded.

Although the appearance of the second phase, $Bi_2Ti_2O_7$, may suppress the dielectric permittivity, the increase of ΔT_1 and ΔT_2 for the samples with $x > 0.14$ points out for the existence of another contribution to the diffuseness in this range. As can be seen in Table 1, the grain size significantly decreases as the amount of Bi doping increases, from 4.0 μm for pure $(Sr_{0.8}Ba_{0.2})TiO_3$ to 0.7 μm for 18 at % Bi doped sample, pointing to a possible dependence of ΔT_1 and ΔT_2 on the grain size.

To confirm the above suggestion, a long time sintering (28 h at 1150°C) was conducted for the $x = 0.16$ composition in an attempt to obtain bigger grains. No evident difference was observed in the X-ray diffraction patterns between the samples sintered for 4 h and for 28 h, but the grain size significantly increased after long time sintering, from 0.6 μm for 4 h to 1.5 μm for 28 h.

The dielectric properties of the samples sintered for 28 h together with the diffuseness parameters (ΔT_1 and ΔT_2) and relaxation parameter (ΔT_3) are shown in Table 1. For the long sintering time there was a slight shift in $T_{\max}$ and a slight increase in $\varepsilon_{r\max}$; ΔT_1 and ΔT_2 decreased significantly while ΔT_3 maintained the same value. These results confirm that the high ΔT_1 and ΔT_2 values attained by the samples with $x > 0.14$ are mainly due to their fine grain structures and that the grain size does not contribute to the frequency dispersion.

It is known that the dielectric properties of $BaTiO_3$ ceramics significantly depend on the grain size [28–32]. For very fine $BaTiO_3$ (grain size $< 1\ \mu$m), the room temperature structure is cubic and the dielectric permittivity peak becomes round, i.e., the phase transition gets diffused. The grain size dependence of ΔT_1 and ΔT_2 presented here indicates that the ferroelectric-paraelectric phase transition of Bi doped $(Sr_{0.8}Ba_{0.2})TiO_3$ gets more diffused by decreasing the grain size to $< 1\ \mu$m, a similar behavior to that observed in $BaTiO_3$.

Although the effects of grain size on the dielectric properties of $BaTiO_3$ ceramics has been widely reported, an understanding of the origin of the diffuse phase transition originated by small grain size has not been completely established. Buessem [29] suggested that the variation of the dielectric properties in fine-grained $BaTiO_3$ ceramics is due to the absence of 90° twinning within the grains, giving rise to internal stresses as the ceramic cools below the Curie temperature. It was further suggested by Martirena et al. [30] that when the grain size decreases, the mobility of the domain walls will decrease, suppressing the dielectric permittivity maximum. Whether these explanations apply to Bi doped $(Sr_{0.8}Ba_{0.2})TiO_3$ needs further study.

5. Conclusions

An investigation of X-ray diffraction patterns and scanning electron microscopy of Bi doped $(Sr_{0.8}Ba_{0.2})TiO_3$ showed that the solubility limit of bismuth in $(Sr_{0.8}Ba_{0.2})TiO_3$ ceramics is around 10 at % at 1250°C. The variation of the temperature of the permittivity maximum $(T_{\max})$ with compositions somewhat confirms this solubility limit value. $T_{\max}$ linearly increases up to 10 at % of bismuth and is almost constant thereafter.

Undoped $(Sr_{0.8}Ba_{0.2})TiO_3$ ceramics show a normal ferroelectric behavior, while a relaxor behavior is observed in Bi doped samples within the solubility limit $(x \leq 0.1)$. The degree of the diffuseness and the relaxation of the phase transition increases as the Bi content increases, whereas the permittivity maximum decreases. It is suggested that Bi^{3+} ions located at off-center Sr^{2+} positions and $Bi^{3+} - V''_A$ dipoles set up a

random electric field, originating the relaxor behavior of Bi doped $(Sr_{0.8}Ba_{0.2})TiO_3$.

When the solubility limit is exceeded $(x > 0.1)$, the diffuseness of the phase transition does not change much in the range $0.1 < x \leq 0.14$ and then increases for $x > 0.14$. The relaxation degree is almost constant in all the range. Grain size variations are suggested to be responsible for the variation of the diffuseness.

Acknowledgments

The authors acknowledge the FCT (Portuguese Foundation for Science and Technology) for financial support and one of them Liqin Zhou thanks Praxis XXI for a maintenance grant.

References

1. G.A. Smolenskii, *J. Phys. Soc. Jap.*, **28**, (supplement), 26 (1970).
2. G.A. Smolenskii and A.I. Agranovskaya, *Sov. Phys. Tech. Phys.*, **3**, 1380 (1958).
3. N. Setter and L.E. Cross, *J. Appl. Phys.*, **51**, 4356 (1980).
4. G.A. Smolenskii, A.I. Agranovskaya, and V.A. Isupov, *Sov. Phys. Solid State*, **1**, 907 (1959).
5. Liqin Zhou, P.M. Vilarinho, and J.L Baptista, *Mater. Res. Bull.*, **29**, 1193 (1994).
6. D. Hennings, A. Schnell, and G. Simon, *J. Am. Ceram. Soc.*, **65**, 539 (1982).
7. W.H. Payne and V.J. Tennery, *J. Am. Ceram. Soc.*, **48**, 413 (1965).
8. G.A. Smolenskii, V.A. Isupov, A.I. Agranovskaya, and S.N. Popov, *Sov. Phys. Solid State*, **2**, 2584 (1961).
9. M.P. Harmer, A. Bhalla, B. Fox, and L.E. Cross, *Mater. Lett.*, **2**, 278 (1984).
10. C.A. Randall, D.J. Barber, and R.W. Whatmore, *J. Microscopy*, **145**, 275 (1987).
11. J. Chen, H.M. Chan, and M.P. Harmer, *J. Am. Ceram. Soc.*, **72**, 593 (1989).
12. L.E. Cross, *Ferroelectrics*, **76**, 241 (1987).
13. D. Viehland, J.F. Li, S.J. Jang, and L.E. Cross, *Phys. Rev. B*, **43**, 8316 (1991).
14. V. Westphal, W. Kleemann, and M.D. Glinchuk, *Phys. Rev. Lett.*, **68**, 847 (1992).
15. M.A. Akbas and P.K. Davies, *J. Am. Ceram. Soc.*, **80**, 2933 (1997).
16. K.A. Müller and H. Burkhard, *Phys. Rev. B*, **19**, 3593 (1979).
17. J.G. Bednorz and K.A. Müller, *Phys. Rev. Lett.*, **52**, 2289 (1984).
18. G.I. Skanava, I.M. Ksendzov, V.A. Trigubenko, and V.G. Prokhvatilov, *Sov. Phys. JEPT*, **6**, 250 (1958).
19. A. Cheng, Y. Zhi, P.M. Vilarinho, and J.L. Baptista, *Phys. Rev. B*, **57**, 7403 (1998).
20. V.V. Lemanov, E.P. Smirnova, P.P. Syrnikov, and E.A. Tarakanov, *Phys. Rev. B*, **54**, 3151 (1996).
21. Liqin Zhou, P.M. Vilarinho, and J.L. Baptista, *J. Europ. Ceram. Soc.*, **19**, 2015 (1999).
22. R.D. Shannon, *Acta Cryst.*, **A32**, 751 (1976).
23. Liqin Zhou, P.M. Vilarinho, and J.L. Baptista, unpublished work.
24. J. Toulouse, B.E. Vugmeister, and R. Pattnaik, *Phys. Rev. Lett.*, **73**, 3467 (1994).
25. B.E. Vugmeister and M.D. Glinchuk, *Rev. Mod. Phys.*, **62**, 993 (1990).
26. H.L. Anderson, *AIP Physics Vademecum* (American Institute of Physics, New York, 1981), p. 294.
27. R.D. Shannon, *J. Appl. Phys.*, **73**, 348 (1993).
28. H. Kniepkamp, W. Heywang, and Z. Angew, *Phys.*, **6**, 385 (1954).
29. W.R. Buessen, L.E. Cross, and A.K. Goswami, *J.Am. Ceram. Soc.*, **49**, 33 (1966).
30. H.T. Martirena and J.C. Burfoot, *J. Phys. C: Solid State Phys.*, **7**, 3182 (1974).
31. N.M. Molokhia, M.A.A. Issa, and S.A. Nasser, *J. Am. Ceram. Soc.*, **67**, 289 (1984).
32. M.H. Frey and D.A. Payne, *Phys. Rev. B*, **54**, 3158 (1996).